Epidemiology and Infection

cambridge.org/hyg

Probable transmission routes of the influenza virus in a nosocomial outbreak

S. Xiao[1], J. W. Tang[2,3], D. S. Hui[4], H. Lei[1,5], H. Yu[1] and Y. Li[1]

[1]Department of Mechanical Engineering, The University of Hong Kong, Hong Kong SAR, China; [2]Clinical Microbiology, University Hospitals of Leicester NHS Trust, Leicester, UK; [3]Infection, Immunity, Inflammation, University of Leicester, Leicester, UK; [4]Department of Medicine and Therapeutics, The Chinese University of Hong Kong, Prince of Wales Hospital, Shatin, Hong Kong SAR, China and [5]School of public health (Shenzhen), Sun Yet-Sen University, Shenzhen, China

Original Paper

Cite this article: Xiao S, Tang JW, Hui DS, Lei H, Yu H, Li Y (2018). Probable transmission routes of the influenza virus in a nosocomial outbreak. *Epidemiology and Infection* **146**, 1114–1122. https://doi.org/10.1017/S0950268818001012

Received: 8 January 2018
Revised: 11 March 2018
Accepted: 3 April 2018
First published online: 6 May 2018

Key words:
Fomite; influenza; long-range airborne; multi-route transmission; nosocomial outbreaks

Author for correspondence:
S. Xiao, E-mail: u3002980@hku.hk

Abstract

Influenza is a long-standing public health concern, but its transmission remains poorly understood. To have a better knowledge of influenza transmission, we carried out a detailed modelling investigation in a nosocomial influenza outbreak in Hong Kong. We identified three hypothesised transmission modes between index patient and other inpatients based on the long-range airborne and fomite routes. We considered three kinds of healthcare workers' routine round pathways in 1140 scenarios with various values of important parameters. In each scenario, we used a multi-agent modelling framework to estimate the infection risk for each hypothesis and conducted least-squares fitting to evaluate the hypotheses by comparing the distribution of the infection risk with that of the attack rates. Amongst the hypotheses tested in the 1140 scenarios, the prediction of modes involving the long-range airborne route fit better with the attack rates, and that of the two-route transmission mode had the best fit, with the long-range airborne route contributing about 94% and the fomite route contributing 6% to the infections. Under the assumed conditions, the influenza virus was likely to have spread via a combined long-range airborne and fomite routes, with the former predominant and the latter negligible.

Introduction

With its enormous morbidity and noticeable mortality rates [1], influenza has long been a serious public health issue. Historically, several pandemics such as the Spanish A/H1N1 influenza in 1918, Asian A/H2N2 influenza in 1957, Hong Kong A/H3N2 influenza in 1968, and most recently, A/H1N1pdm09 influenza in 2009 have recurred, killing millions of people and dramatically affecting the economy and society [2–4]. In addition to these pandemics, the influenza virus induces seasonal epidemics every year, resulting in 3–5 million cases of severe illness and approximately 250 000–500 000 deaths worldwide [5].

Despite 70 years of influenza control [6], our understanding of its transmission is still limited [7, 8]. The transmission modes of the influenza virus are controversial [7, 9–12], particularly regarding whether influenza is transmitted via the long-range airborne route, the close contact route, the fomite route or combinations of these routes. The close contact route here includes short-range airborne transmission, direct inhalation of droplet nuclei from the expiratory air stream of the infector and direct deposition of large droplets on the mucous membranes of susceptible individuals. Because of this knowledge gap, the recommendations of non-pharmaceutical interventions from the World Health Organisation (WHO) [5] and the Centers for Disease Control and Prevention (CDC) [11] are aimed at all possible influenza transmission routes. Better knowledge of influenza transmission could promote the development and selection of more appropriate infection control measures in healthcare settings, at workplaces and in homes [7, 8].

To further investigate the transmission modes of the influenza virus, we conducted a mathematical modelling study in a 2008 nosocomial outbreak in Hong Kong [13]. In this outbreak, since the index patient and most other inpatients were bed-bound during their illnesses [13], we excluded the possibility of the close contact transmission between inpatients. On the basis of the other two transmission routes, three kinds of hypotheses of transmission modes were formulated between index patient and other inpatients: single-route long-range airborne transmission (Hypothesis 1 (Long air)), single-route fomite transmission (Hypothesis 2 (Fomite)) and the combined two-route transmission (Hypothesis 3 (Long air + Fomite)). Furthermore, we assumed three representative healthcare workers' (HCWs') routine round patterns, and subdivided Hypotheses 2 and 3 into Hypotheses 2 (Fomite (Pathway 1)), 2 (Fomite (Pathway 2)), 2 (Fomite (Pathway 3)), 3 (Long air + Fomite (Pathway 1)), 3 (Long air + Fomite (Pathway 2)) and 3 (Long air + Fomite (Pathway 3)), respectively. We applied a multi-agent model to simulate how the viruses were transmitted from the index patient to

susceptible people by airflow and surface touching to determine the exposure doses and infection risks. We considered 1140 scenarios with various values of four important parameters and conducted least-squares fitting for each scenario to evaluate the hypotheses by comparing the distribution of the predicted infection risk with that of the reported attack rates [13]. The results provide probable evidence for influenza transmission modes in different scenarios.

Methods

Outbreak

As shown in Figure 1, the outbreak occurred in a general medical ward in the Prince of Wales Hospital in Hong Kong in March and April 2008 [13]. According to the identical viral sequencing results [13], all the secondary cases were assumed to be due to a single index patient, a 68-year-old man who developed symptoms of an acute exacerbation of chronic obstructive pulmonary disease on 27 March and was admitted to Bed 24 in the ward. He was bed-bound (i.e. was non-ambulatory and unable to walk around the ward by himself) since hospitalisation due to respiratory failure and required non-invasive positive pressure ventilation (NPPV) in the evening on 31 March 2008 as his condition deteriorated with increasing respiratory distress. It was therefore assumed that this index patient acted as a single, 'static' source for this outbreak.

On 1 April, he was transferred to the intensive care unit for invasive (i.e. closed circuit) mechanical ventilation; the influenza H3N2 (Influenza A/Brisbane/10/2007) virus was later isolated from a tracheal aspirate sample [13]. Thus, the period from 27 to 31 March 2008 was taken as the potential exposure period.

The outbreak ward contained a common patients' toilet, a long corridor and three bays, consisting of 28 beds (Beds 1–8 in Bay A, Beds 9–18 in Bay B and Beds 19–28 in Bay C). The adjacent beds were about 1 m apart. Three high-efficiency particulate absorbing (HEPA) air purifiers were positioned at the wall end of the three bays, along with four fan-coil units (one in each bay and one over the nurses' station) and four return air grills in the corridor. All HEPA filters were assumed to function with 100% filtration of the modelled droplet nuclei [13]. The measured airflow rates in the ward are shown in Figure 1. During the outbreak, the HEPA air purifiers in Bays A and B were set to 'low' and that in Bay C was set to 'medium', with injection velocity 1.47, 1.44 and 1.90 m/s, respectively [13].

In this research, we identified people in six representative roles (inpatients, visitors, doctors, nurses, health assistants and cleaners) as the study objects and focused on the infection patterns of the inpatients in the three bays. We assumed that all exposure doses received by the susceptible patients came from the index patient due to his respiratory activities, such as coughing. As shown in Figure 2a, c and e, we assumed three representative HCWs' routine round pathways. In Pathway 1 (Fig. 2a), HCWs were responsible for all inpatients and examined them in the ward in a clockwise direction. In Pathway 2 (Fig. 2c), each doctor and each nurse were responsible for the inpatients in a bay and examined them in a clockwise or anticlockwise direction. In Pathway 3 (Fig. 2e), each doctor and each nurse allocated the patients in the order in which they arrived and thus, examined a random set of nine or ten inpatients (as denoted by the circles of three different colours) in the ward in a clockwise direction.

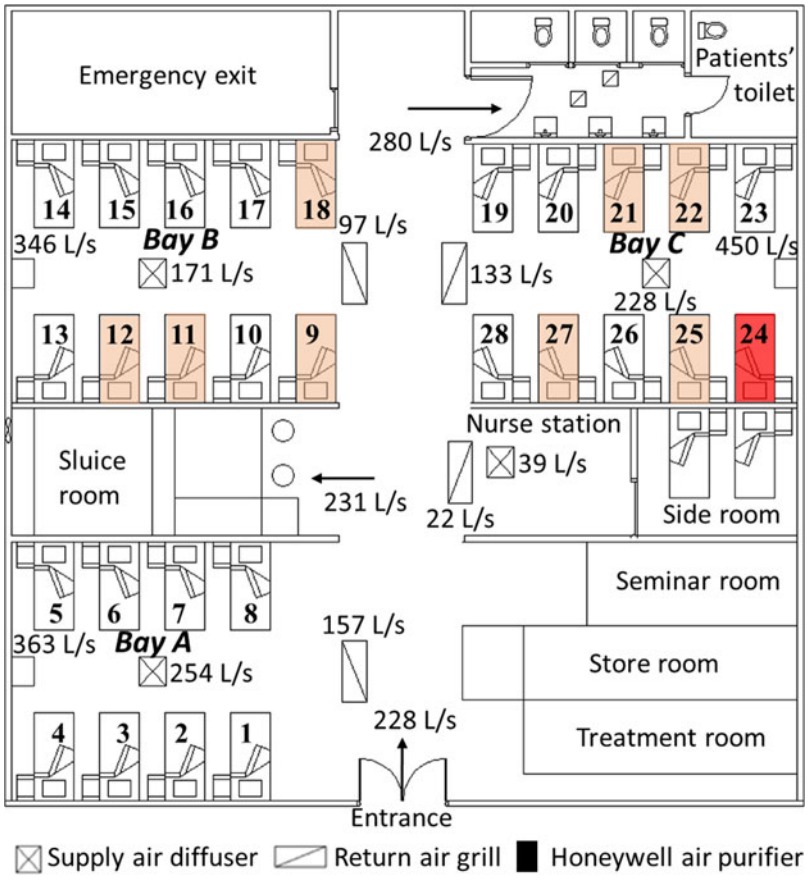

Fig. 1. Floor plan of the outbreak ward and the measured airflow rates (*L*/s) at different locations [13]. The bed (No. 24) of the index patient is marked in red and the beds (Nos. 9, 11, 12, 18, 21, 22, 25 and 27) of the infected patients are marked in pink.

https://doi.org/10.1017/S0950268818001012

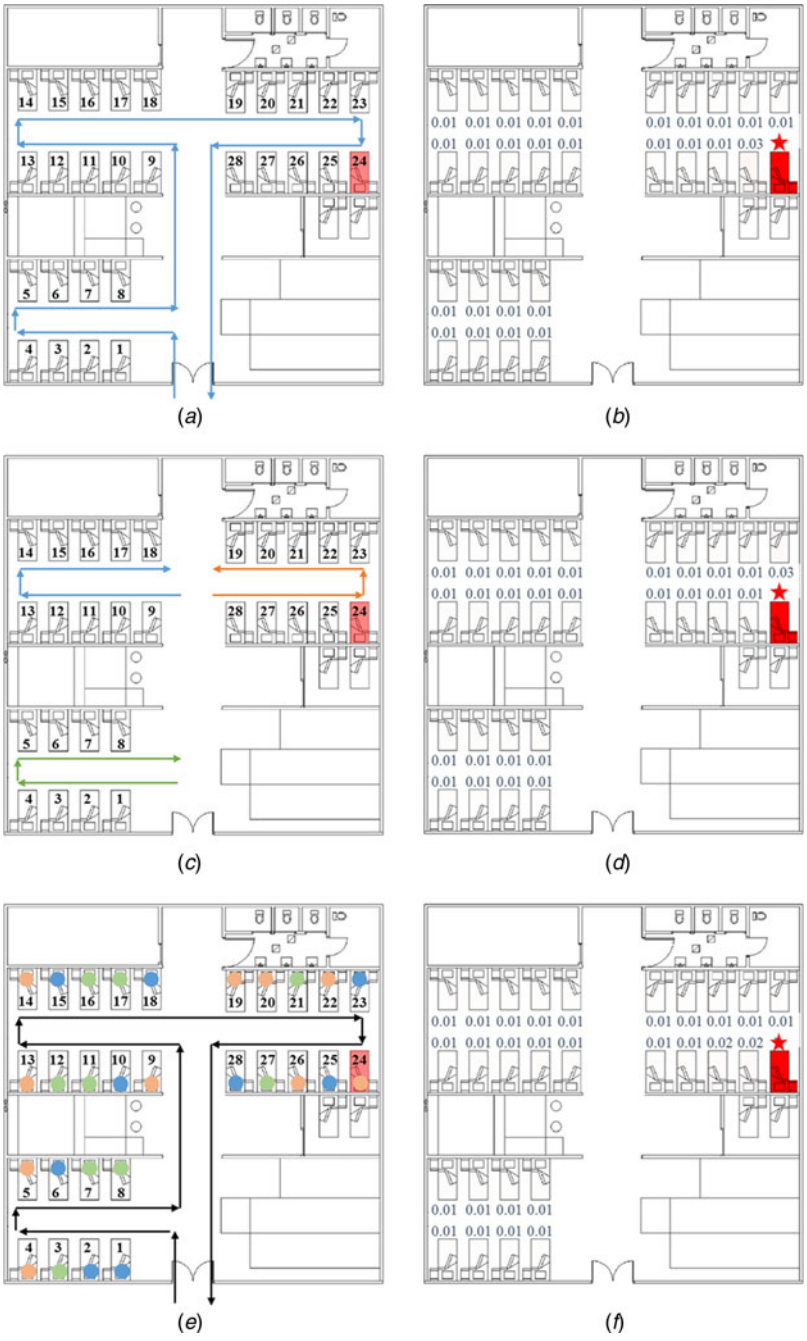

Fig. 2. Healthcare workers' (HCWs') routine round patterns and predicted infection risks. (a) HCWs' routine patient care contact Pathway 1. (b) Predicted average infection risk distribution (for 1000 simulations) via the fomite route (Pathway 1) at 24:00 on 31 March, the end of the exposure period. (c) HCWs' routine patient care contact Pathway 2. (d) Predicted average infection risk distribution via the fomite route (Pathway 2). (e) HCWs' routine patient care contact Pathway 3. (f) Predicted average infection risk distribution via the fomite route (Pathway 3). The largest virus-containing droplet size $d_g = 200$ μm, the dose-response parameters in the respiratory tract $\alpha_r = 1.03/\text{TCID}_{50}$ and on mucous membranes $\alpha_m = 0.0014/\text{TCID}_{50}$ and the viral load $L_0 = 10^9$ TCID_{50}/ml. The predicted average infection risk for every inpatient is marked in (b), (d) and (f). The bed marked with a star represents that of the index patient.

During the hospitalisation of the index patient, eight of the 59 inpatients were infected by the same H3N2 virus subtype (Influenza A/Brisbane/10/2007), as determined by nucleotide sequence analysis. The distribution of the infected inpatients is shown in Figure 1, with the highest attack rate (0.222; four of 18 inpatients) in the adjacent cubicle (Bay B) and a slightly lower rate (0.200; four of 20 inpatients) in the source cubicle (Bay C); no patients were infected in the remote cubicle (Bay A) [13].

Multi-agent modelling framework

A multi-agent modelling framework [14, 15] was used to calculate the infection risk of the inpatients from the three hypothesised influenza transmission modes described above. The mathematical model was implemented in MATLAB R2014a (Mathworks, USA). In this framework, we considered 18 types of representative surfaces (Supplementary Table S2) and categorised them into five types of material according to their properties: porous surfaces, non-porous surfaces, toilet surfaces, skin and mucous membranes in the eyes, noses and mouths (Supplementary Table S2). For the different roles of people studied, we considered various types of behaviours; the frequencies and the sequences of touching were assumed and are summarised in Supplementary Tables S7 and S8, respectively.

Further, in the above framework, three mathematical models were applied to calculate the amount of exposure. For the long-range airborne route, a multi-zone model [14–17] was used to acquire the aerosol concentrations in the six zones of the outbreak

https://doi.org/10.1017/S0950268818001012

ward (Supplementary Fig. S1), and a long-range airborne route exposure model [14, 15] was used to calculate the exposure doses in the respiratory tract. For the fomite route, a surface contamination model [14, 15, 18] was used to calculate the virus concentration on multiple environmental surfaces and the exposure doses on the mucous membranes. With the obtained exposure doses, a dose–response relationship model [14, 15, 18–20] was used to calculate the infection risk.

As in previous studies [14, 15], we identified some important but uncertain parameters, including the largest virus-containing droplet size d_g, dose–response parameters in the respiratory tract α_r and on the mucous membranes α_m, and the viral load L_0. To reduce the number of variables, α_r, α_m and L_0 were combined as the products $\alpha_r L_0$ and $\alpha_m L_0$, which are defined as the dose effects of introducing 1 ml of virus-laden droplets with a viral load of L_0 into the respiratory tract and the mucous membranes, respectively. On the basis of the existing literature, we investigated the ranges of three parameters: d_g (four values: 20, 50, 100 and 200 μm), $\alpha_r L_0$ (21 values: 10^5–10^{10}/ml) and $\alpha_m L_0$ (21 values; 10^2–10^7/ml). In this study, we considered 1140 scenarios with different value combinations of the parameters ($\alpha_r L_0$, $\alpha_m L_0$, d_g) and ran simulations 1000 times for each scenario.

In each scenario, according to the dose–response relationship model [14, 15, 18–20], the infection risk I was calculated as [15].

$$I = 1 - e^{-c_a \alpha_r D_a(d_g,\ L_0) - c_f \alpha_m D_f(d_g,\ L_0)}$$

where c_a equals 1 if the long-range airborne route exists and 0 otherwise, and c_f is the indicator for the fomite route. The exposure dose due to the long-range airborne route D_a and that due to the fomite route D_f are functions of d_g and L_0.

Least-squares fitting

To evaluate each transmission hypothesis, we compared the spatial distribution of the infection risk under each hypothesis to the reported attack rates. In this study, we chose a statistical approach, maximising fit, to select the probable hypothesis [21]. In particular, we used the least-squares fitting method, which takes the residual sum of squares (RSS) as a measure of fit [22]. Because a small RSS indicates a good fit of the model to the data, the hypothesis with the minimum RSS was regarded as a probable explanation to the outbreak [15].

Results

Spatial patterns of the predicted infection risk

The average infection risk distributions of 1000 simulations at the end of the exposure period via fomite routes (three patterns) and the long-range airborne are shown in Figures 2b, d, f and 3b, respectively. In these distributions, the values of parameters ($\alpha_r L_0$, $\alpha_m L_0$, d_g) were set to be the same.

For the long-range airborne route, the infection risk was the highest in Bay C (the source cubicle), lower in Bay B (the adjacent cubicle) and the lowest in Bay A (the remote cubicle), which is consistent with the virus concentration distributions obtained from computational fluid dynamics (CFD) simulations [13] and multi-zone modelling methods (Fig. 3a). Virus-containing aerosols were generated during the index patient's respiratory therapy with NPPV, so the virus concentration was the highest in the source cubicle. According to the locations of the supply air diffusers and the return air grills shown in Figure 1, the cubicles had positive pressure towards the corridor. Nevertheless, because of the small temperature difference, two-way airflow patterns occurred at the opening between the corridor and the cubicles, leading to a significant air exchange between the corridor and the cubicles [23]. Moreover, the bed of the index patient was right next to a HEPA air purifier in the source cubicle, and this purifier had a higher air injection velocity than that in the adjacent cubicle, leading to more contaminated air being pushed into the corridor and the adjacent cubicle [13]. Thus, the virus-containing aerosols spread to the other areas of the ward with the airflows. Because the air in the remote cubicle was more diluted than that in the adjacent cubicle, the airborne droplet concentration (Fig. 3a) and infection risk (Fig. 3b) were the lowest in the remote cubicle. Since the filtration efficiency of HEPA air purifiers was about 100%, the overall infection risk was not high, and the difference between the infection risk in the source ward and that in the remote ward was large (Fig. 3b), which was consistent with CFD simulations in a similar hospital ward [24].

For the fomite route, the infection risk for all susceptible people was very low. In hospital wards, the transmission of the virus via the fomite route depends mainly upon the HCWs' hands and the environmental surfaces [14, 15]. Because of the rapid natural inactivation rates on the skin (Supplementary Table S4), the contribution of HCWs' hands to the infection was very low; therefore, the routine care pathways of the HCWs would have had very little effect on the infection risk distributions, except for a few patients who were specifically visited by HCWs after the index patient (Bed 25 in Fig. 2b, Bed 23 in Fig. 2d and Beds 25 and 26 in Fig. 2f). Thus, the common environmental surfaces, such as those in the toilets, played a predominant role in spreading the virus via the fomite route. Because all susceptible people had the same opportunity to touch the common surfaces, they were expected to receive equivalent exposures from the common surfaces. Thus, the average infection risk of 1000 simulations was equivalent for most of the susceptible people.

Predicted distributions with the best fitness

Table 1 shows scenarios with the best fitness (the minimum RSS) for the hypotheses. Among the single-route modes, Hypothesis 1 (Long air) had the best fitness because it could predict the infection risk quantitatively as compared to the attack rates. The fitness of Hypothesis 2 (Fomite) was poor for all of the three pathways because the infection risk via the fomite route was very small, which deviated largely from the attack rates in all the scenarios. Thus, a higher infection risk via the fomite route would lead to better fitness, so in scenarios with the best fitness for the hypotheses related to the fomite route (Hypotheses 2 and 3 in Table 1), the largest virus-containing droplet size is 200 μm, the largest value assumed for the parameter.

As shown in Table 1, hypotheses involving the long-range airborne route (Hypotheses 1 and 3) had better fitness than others, and the role of the long-range airborne route was always predominant. From Table 1, the reported attack rate in adjacent ward (Bay B) was actually larger than the source ward (Bay C) while the predicted infection risk of the long-range airborne route in Bay B was much smaller than that in Bay C. Since the predicted infection risk of the fomite route in Bay B was similar to that in Bay C, the combination of the two routes (namely Hypothesis 3) would have better fitness than the single routes. Compared

https://doi.org/10.1017/S0950268818001012

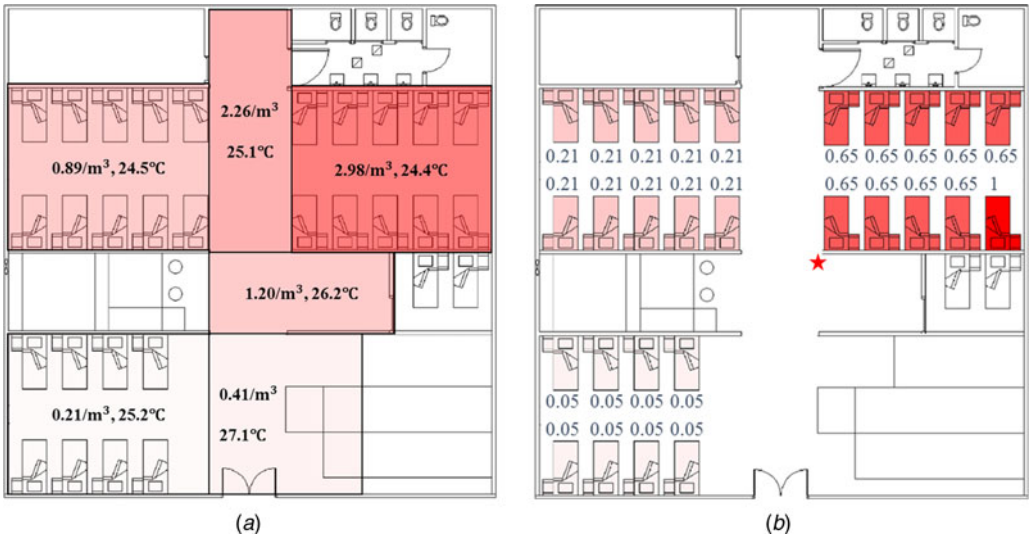

Fig. 3. Distributions of airborne droplets and predicted infection risk. (a) Distributions of airborne droplets (number/m^3) and temperature (°C) obtained using multi-zone methods. (b) Predicted average infection risk distribution (for 1000 simulations) via the long-range airborne route at 24:00 on 31 March, the end of the exposure period. The largest virus-containing droplet size d_g = 200 μm, the dose-response parameters in the respiratory tract α_r = 1.03/TCID$_{50}$ and on mucous membranes α_m = 0.0014/TCID$_{50}$ and the viral load $L_0 = 10^9$ TCID$_{50}$/ml. The predicted average infection risk for every inpatient is marked in (b). The bed marked with a star represents that of the index patient.

with the other two pathways, Hypothesis 3 (P2) resulted in the prediction most consistent to the attack rates. In the transmission, the long-range airborne route contributed approximately 94% to the infection risk, whilst the fomite route only contributed about 6%.

Figure 4 shows the hypotheses with the best fitness (i.e. the minimum RSS) in the 1140 scenarios. In scenarios with d_g of 20 μm (Fig. 4a), all virus-containing droplets were very small and could remain suspended in the air for a long time. The deposition of virus-containing droplets on the surfaces was severely weakened, which leads to the negligible infection risk via the fomite route. Thus, no hypotheses related to the fomite route are shown in Figure 4a.

In scenarios with d_g of 50, 100 and 200 μm (Fig. 4b–d), since d_g was larger than the largest initial diameter for the airborne droplets (30 μm), the infection risk via the long-range airborne route was irrelevant to d_g. Moreover, the exposure site for this route was in the respiratory tract, so the infection risk was not related to α_m. For the fomite route, the infection risk was low for all scenarios and thus varied slightly with parameters ($\alpha_r L_0$, $\alpha_m L_0$, d_g).

Table 1. Scenarios with the best fitness (minimum residual sum of squares, RSS) for Hypotheses 1 (Long air), 2 (Fomite (Pathway 1)), 2 (Fomite (Pathway 2)), 2 (Fomite (Pathway 3)), 3 (Long air + Fomite (Pathway 1)), 3 (Long air + Fomite (Pathway 2)) and 3 (Long air + Fomite (Pathway 3))

		Hypothesis						
Parameter	Reported data	1	2 (P1)	2 (P2)	2 (P3)	3 (P1)	3 (P2)	3 (P3)
Minimum RSS	N.A.	0.514	1.553	1.565	1.559	0.510	0.505	0.508
d_g[a] (μm)	Unknown	20	200	200	200	200	200	200
$\alpha_r L_0$[b] (/ml)	Unknown	$10^{9.00}$	–	–	–	$10^{8.50}$	$10^{8.50}$	$10^{8.50}$
$\alpha_m L_0$[b] (/ml)	Unknown	–	$10^{7.00}$	$10^{7.00}$	$10^{7.00}$	$10^{7.00}$	$10^{7.00}$	$10^{7.00}$
Average infection risk								
Source ward (Bay C)	0.200	0.268	0.010	0.008	0.009	0.280	0.279	0.279
Adjacent ward (Bay B)	0.222	0.070	0.008	0.008	0.008	0.079	0.079	0.079
Remote ward (Bay A)	0.000	0.016	0.008	0.008	0.008	0.024	0.024	0.024
Overall	0.136	0.118	0.008	0.008	0.008	0.127	0.127	0.127
Relative contribution								
Long-range airborne route	Unknown	100%	0	0	0	93.5%	93.9%	93.9%
Fomite route	Unknown	0	100%	100%	100%	6.5%	6.1%	6.1%

[a]d_g denotes the largest virus-containing droplet size.
[b]$\alpha_r L_0$ and $\alpha_m L_0$ denote the products of the viral load and the dose–response parameters in the respiratory tracts and on the mucous membranes, respectively.

https://doi.org/10.1017/S0950268818001012

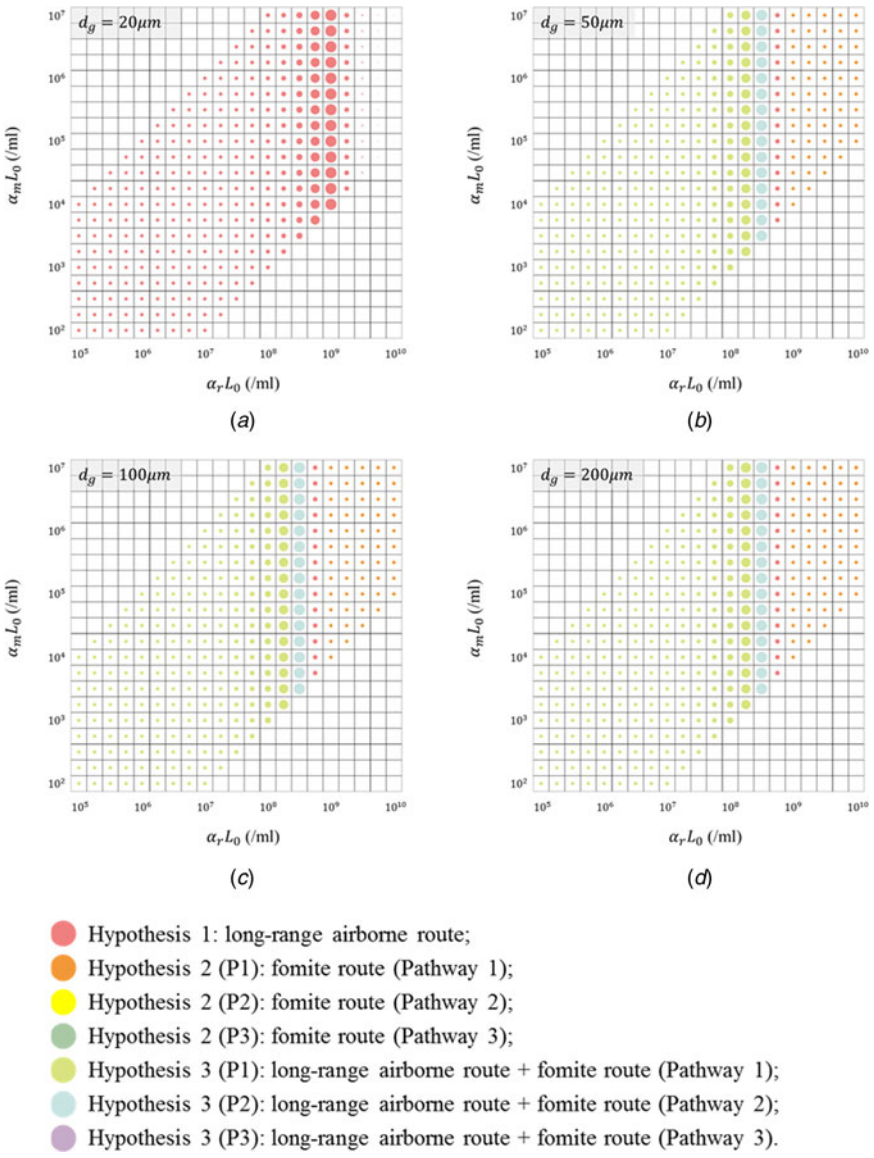

Fig. 4. Illustration of the hypotheses with the best fitness (minimum residual sum of squares; RSS) for the 1140 scenarios, with different values for the largest virus-containing droplet size d_g (20, 50, 100 and 200 μm) and products of viral load and dose–response parameters in respiratory tracts $\alpha_r L_0$ (21 values, 10^5–10^{10}/ml) and on mucous membranes $\alpha_m L_0$ (21 values, 10^2–10^7/ml). (a) $d_g = 20$ μm; (b) $d_g = 50$ μm; (c) $d_g = 100$ μm; (d) $d_g = 200$ μm. Different hypotheses are marked with different-coloured dots. The dot diameter is inversely proportional to the value of the RSS.

Therefore, in Fig. 4b–d, the results varied considerably with $\alpha_r L_0$ but changed little with d_g and $\alpha_m L_0$. When $\alpha_r L_0$ was small and moderate, the infection risk caused by any single-route mode was small, and then the probable transmission modes were Hypothesis 3 (Long air + Fomite) (cyan and blue dots). When $\alpha_r L_0$ were large, the probable transmission modes were single-route ones (red and orange dots), but the corresponding fitness was very poor.

Discussion

Although the actual values of parameters ($\alpha_r L_0$, $\alpha_m L_0$, d_g) in the outbreak were unknown, some more-likely values could be identified based on the literatures. Despite not always detectable [25], influenza viruses have been found in human saliva [26] where large droplets originate [27], so the largest virus-containing droplet size d_g is more likely to be 50, 100 and 200 μm. The viral shedding varied with people [28], and Nicas and Jones estimated the virus concentration ranged from 10^4 to 10^8 $TCID_{50}$/ml [19] based on the measurements of Murphy *et al.* [29]. According to Spicknall *et al.* [30], we estimated the dose–response parameter of influenza in the respiratory tract α_r as $1.03/TCID_{50}$ and that on mucous membranes α_m as $1.4 \times 10^{-3}/TCID_{50}$. Thus, the product $\alpha_r L_0$ was more likely to range from 1.03×10^4 to 1.03×10^8/ml, and $\alpha_m L_0$ was more likely to range from 1.4×10^1 to 1.4×10^5/ml. From Fig. 4b–d, with these more-likely parameter values, the probable transmission mode was Hypothesis 3 (Long air + Fomite (P1)), but the fitness with the reported attack rates (RSS = 0.929) was not good. If the index patient shed a higher viral load than average and the product $\alpha_r L_0$ increased to $10^{8.50}$/ml, the probable transmission mode was Hypothesis 3 (Long air + Fomite (P2)) and the fitness (RSS = 0.520) was almost as good as the overall best fitness (RSS = 0.505) in Table 1.

As the above analyses suggest, whether the index patient shed an average viral load comparable to those reported in literatures or the index patient was a super-spreader, the influenza virus was most probably spread via a combined long-range airborne and fomite transmission mode in the considered outbreak. The potential of the two transmission routes has been supported by the detection of influenza virus ribonucleic acid (RNA) in the air [31, 32] and

https://doi.org/10.1017/S0950268818001012

on surfaces [33, 34] in indoor environments. Additional data have demonstrated that the influenza virus can survive for several hours in the air [35, 36] and on fomites [37, 38].

As the results show, it is most likely that in this outbreak, the long-range airborne route made a predominant contribution to the influenza infections [13], which the original study authors also suggested. Moreover, the current modelling study suggests the fomite transmission route played a slight role. The relative importance of these two routes suggested by our results could explain the following findings: ultraviolet radiation [39] and ventilation [40, 41] significantly affected the attack rates in some influenza outbreaks, whilst little or no direct evidence has been found to show that fomites can mediate transmission [8] despite the emphasis on hand-washing and surface cleaning. In addition, several control measures aimed at reducing the aerosol transmission achieved a good effect in the hospital after the outbreak [13], which also supported the significant role of the long-range airborne route. As the original outbreak investigation [13] reported, a series of measures were applied, such as isolating patients with suspected influenza, usage restriction of aerosol-generating procedures, regular checking on air-conditioning units and settings and the use of N-95 respirators. As a result, the hospital did not encounter another influenza outbreak in open wards during the subsequent year, including the first wave of the influenza H1N1 pandemic in 2009.

Other modelling investigations [19, 30, 42, 43] have been performed to quantify the relative importance of different routes in influenza transmission. Similar to this study, Atkinson and Wein [42] and Lei *et al.* [43] concluded that the airborne route is far more dominant than the fomite route. Nicas and Jones [19] and Spicknall *et al.* [30] predicted a substantial contribution of the fomite route to the infection. In their assumptions, the virus source of the fomite route included the large droplets and the virus concentrations in large droplets were the same with small ones. In contrast, on the basis of the absence of any detectable influenza RNA in naturally infected human volunteer exposure experiments, Tang *et al.* [25] speculated that large droplets produced during human exhalations (breathing and coughing) may not carry a significant amount of virus because they may consist of less viscous, less virus-rich salivary fractions, whereas most of the virus may remain trapped in the mouth within more viscous salivary mucins that contain antiviral substances. Therefore, for various reasons, the contribution of the fomite route may have been overestimated in these two studies [19, 30].

The general ward in which this outbreak occurred is similar to that in which the largest severe acute respiratory syndrome (SARS) nosocomial outbreak in Hong Kong [14] occurred. The cubicles in these wards were all designed to maintain positive pressure relative to the corridor, but the virus-containing airborne droplets could still spread from the source cubicle to other cubicles because of the two-way airflow effect [23]. In the nosocomial outbreaks of SARS [14] and influenza [13] on the general medical ward, there was very likely a significant contribution by the application of a jet nebuliser and NPPV on the index patients respectively in addition to an imbalanced ward airflow. In experimental studies using smoke particles as exhaled air marker, application of a jet nebuliser or NPPV on a human patient simulator via a single circuit and various face masks has been shown to produce significant leakage and room contamination even in an isolation room with negative pressure [44–46]. Therefore, the long-range airborne route played a predominant role in the virus transmission in these two outbreaks [13, 14]. Chen *et al.* [23] suggested that reducing the area of the openings between the cubicles and the corridor would help to reduce the potential for long-range airborne transmission. Unlike in this influenza outbreak, the fomite route made a considerable contribution to the infection in the SARS outbreak. The difference could be attributed to virus inactivation rates on surfaces, particularly hands. The inactivation rate of the SARS virus on hands was estimated to be 0.80/h on the basis of the measurement of the 229E coronavirus [47] and that of influenza viruses was estimated to be 55/h [30, 37], which implies that approximately 1.3% of the SARS viruses and 60% of the influenza viruses are inactivated every minute. Thus, most of the influenza viruses transmitted to the hands of the HCWs during contact with the index patient might be inactivated before the HCWs can transmit them to subsequent inpatients and before the subsequent inpatients can then touch their own mucous membranes. Hence, the fomite route appears to be of less importance for the transmission of the influenza virus [10].

This study has the following three limitations. First, because the knowledge of some aspects of the influenza virus is still limited, some parameters of the model are uncertain, such as the transfer rates between hands and surfaces (Supplementary Table S3). In this study, we discussed only the range of possible values of some important parameters ($\alpha_r L_0$, $\alpha_m L_0$, d_g) and used published estimates for other parameters, sometimes based on other non-influenza viruses, bacteriophages or even bacteria, which could lead to less accurate results.

Second, because of a lack of detailed and contemporaneous information during the outbreak, most of the patient and staff behaviours during the outbreak were assumed, retrospectively. Nevertheless, human behaviours are to some extent crucial for constructing multi-agent models, since they can affect the infection risk generated for each of the two transmission routes. For example, the duration and frequency of the index patient walking in the corridor would influence the virus source strengths of the two routes. Moreover, the individual variation in the behavioural modes of people performing the same roles were not considered in this study; for example, nurses were assumed to visit all normal inpatients at the same frequency, which is unlikely in reality because the most sick patients will usually receive the maximum attention, thereby relatively influencing virus transmission via the fomite route.

Third, the patient-to-patient close contact transmission was not considered in this study. The close contact route, in particular the large droplet route, has long been perceived to be the most important in the influenza transmission [5, 11, 48–50]. However, in this outbreak, since the index patient and most other inpatients were immobile during their illnesses [13], the possibility of direct contact between the index patient and other inpatients was nearly impossible. In addition, the distance between the patient in the adjacent bed and the index patient was about 2 m [13], and the index patient was less likely to cough or sneeze in the direction of the adjacent beds since he initially required supplemental oxygen via nasal cannula and then underwent BiPAP (bi-level positive airway pressure) ventilation support. Thus, the close contact transmission might have made little contribution to the overall infection patterns so it was ignored in this study.

Overall, more laboratory measurements and human behaviour observations in hospitals are needed for a better understanding of influenza transmission.

https://doi.org/10.1017/S0950268818001012

Conclusions

In this outbreak, the influenza virus might have spread via a transmission mode involving the long-range airborne route. This virus was probably transmitted via the combined two-route mode and HCWs might have conducted the routine rounds in Pathways 1 or 2. In the two-route mode, the long-range airborne route played a predominant role and the fomite route played a very small role. Our findings on the influenza transmission modes and the possible roles of the two routes contribute to the development of evidence-based infection control advice for healthcare settings.

Supplementary material. The supplementary material for this article can be found at https://doi.org/10.1017/S0950268818001012.

Acknowledgements. This work was supported by an HKSAR Government Collaborative Research Fund project (grant number C7025-16G) and a General Research Fund project (grant number 17211615).

Declaration of interest. None.

Ethical standards. No ethics approval was required for this study as this is a reanalysis of a past outbreak.

References

1. **Monto AS** (1987) Influenza: quantifying morbidity and mortality. *The American Journal of Medicine* **82**, 20–25.
2. **Potter CW** (2001) A history of influenza. *Journal of Applied Microbiology* **91**, 572–579.
3. **World Health Organization** (2005) Ten things you need to know about pandemic influenza (update of 14 October 2005). *The Weekly Epidemiological Record* **80**, 428–431.
4. **Dawood FS, *et al.*** (2012) Estimated global mortality associated with the first 12 months of 2009 pandemic influenza A H1N1 virus circulation: a modelling study. *The Lancet Infectious Diseases* **12**, 687–695.
5. **Fact sheet on seasonal influenza.** Available at http://www.who.int/mediacentre/factsheets/fs211/en/ (Accessed 20 August 2017).
6. **70 years of influenza control.** Available at http://www.who.int/influenza/gip-anniversary/en/ (Accessed 23 August 2017).
7. **Brankston G, *et al.*** (2007) Transmission of influenza A in human beings. *The Lancet Infectious Diseases* **7**, 257–265.
8. **Killingley B and Nguyen-Van-Tam J** (2013) Routes of influenza transmission. *Influenza and Other Respiratory Viruses* **7**, 42–51.
9. **Tellier R** (2006) Review of aerosol transmission of influenza A virus. *Emerging Infectious Diseases* **12**, 1657–1662.
10. **Weber TP and Stilianakis NI** (2008) Inactivation of influenza A viruses in the environment and modes of transmission: a critical review. *Journal of Infection* **57**, 361–373.
11. **Prevention strategies for seasonal influenza in healthcare settings: guidelines and recommendations.** Available at https://www.cdc.gov/flu/professionals/infectioncontrol/healthcaresettings.htm (Accessed 23 August 2017).
12. **Zhang N, *et al.*** (2016) Dynamic population flow based risk analysis of infectious disease propagation in a metropolis. *Environment International* **94**, 369–379.
13. **Wong BCK, *et al.*** (2010) Possible role of aerosol transmission in a hospital outbreak of influenza. *Clinical Infectious Diseases* **51**, 1176–1183.
14. **Xiao S, *et al.*** (2017) Role of fomites in SARS transmission during the largest hospital outbreak in Hong Kong. *PLoS ONE* **12**, e0181558.
15. **Xiao S, *et al.*** (2018) A study of probable transmission routes of MERS-CoV in the first hospital outbreak in the Republic of Korea. *Indoor Air* **28**, 51–63.
16. **Li Y, Delsante A and Symons J** (2000) Prediction of natural ventilation in buildings with large openings. *Build and Environment* **35**, 191–206.
17. **Li Y, *et al.*** (2005) Multi-zone modeling of probable SARS virus transmission by airflow between flats in Block E, Amoy Gardens. *Indoor Air* **15**, 96–111.
18. **Xiao S, Tang JW and Li Y** (2017) Airborne or fomite transmission for norovirus? A case study revisited. *International Journal of Environmental Research and Public Health* **14**, 1571.
19. **Nicas M and Jones RM** (2009) Relative contributions of four exposure pathways to influenza infection risk. *Risk Analysis* **29**, 1292–1303.
20. **Zhang N, *et al.*** (2018) A human behavior integrated hierarchical model of airborne disease transmission in a large city. *Building and Environment* **127**, 211–220.
21. **Johnson JB and Omland KS** (2004) Model selection in ecology and evolution. *Trends in Ecology & Evolution* **19**, 101–108.
22. **Draper NR, Smith H and Pownell E** (1966) *Applied Regression Analysis*. New York: Wiley.
23. **Chen C, *et al.*** (2011) Role of two-way airflow owing to temperature difference in severe acute respiratory syndrome transmission: revisiting the largest nosocomial severe acute respiratory syndrome outbreak in Hong Kong. *Journal of the Royal Society Interface* **8**, 699–710.
24. **Qian H, *et al.*** (2009) Spatial distribution of infection risk of SARS transmission in a hospital ward. *Building and Environment* **44**, 1651–1658.
25. **Tang JW, *et al.*** (2014) Absence of detectable influenza RNA transmitted via aerosol during various human respiratory activities – experiments from Singapore and Hong Kong. *PLoS ONE* **9**, e107338.
26. **Endo T, *et al.*** (2010) Reflectometric detection of influenza virus in human saliva using nanoimprint lithography-based flexible two-dimensional photonic crystal biosensor. *Sensors and Actuators B: Chemical* **148**, 269–276.
27. **Johnson G, *et al.*** (2011) Modality of human expired aerosol size distributions. *Journal of Aerosol Science* **42**, 839–851.
28. **Yan J, *et al.*** (2018) Infectious virus in exhaled breath of symptomatic seasonal influenza cases from a college community. *Proceedings of the National Academy of Sciences of the United States of America* **115**, 1081–1086 .
29. **Murphy BR, *et al.*** (1973) Temperature-sensitive mutants of influenza virus. III. Further characterization of the ts-1 [E] influenza A recombinant (H3N2) virus in man. *Journal of Infectious Diseases* **128**, 479–487.
30. **Spicknall IH, *et al.*** (2010) Informing optimal environmental influenza interventions: how the host, agent, and environment alter dominant routes of transmission. *PLoS Computational Biology* **6**, e1000969.
31. **Blachere FM, *et al.*** (2009) Measurement of airborne influenza virus in a hospital emergency department. *Clinical Infectious Diseases* **48**, 438–440.
32. **Yang W, Elankumaran S and Marr LC** (2011) Concentrations and size distributions of airborne influenza A viruses measured indoors at a health centre, a day-care centre and on aeroplanes. *Journal of the Royal Society Interface* **8**, 1176–1184.
33. **Boone SA and Gerba CP** (2005) The occurrence of influenza A virus on household and day care center fomites. *Journal of Infection* **51**, 103–109.
34. **Simmerman JM, *et al.*** (2010) Influenza A virus contamination of common household surfaces during the 2009 influenza A (H1N1) pandemic in Bangkok, Thailand: implications for contact transmission. *Clinical Infectious Diseases* **51**, 1053–1061.
35. **Loosli C, *et al.*** (1943) Experimental air-borne influenza infection. I. Influence of humidity on survival of virus in air. *Proceedings of the Society for Experimental Biology and Medicine* **53**, 205–206.
36. **Schaffer F, Soergel M and Straube D** (1976) Survival of airborne influenza virus: effects of propagating host, relative humidity, and composition of spray fluids. *Archives of Virology* **51**, 263–273.
37. **Bean B, *et al.*** (1982) Survival of influenza viruses on environmental surfaces. *The Journal of Infectious Diseases* **146**, 47–51.
38. **Noyce J, Michels H and Keevil C** (2007) Inactivation of influenza A virus on copper versus stainless steel surfaces. *Applied and Environmental Microbiology* **73**, 2748–2750.
39. **McClean R** (1961) The effect of ultraviolet radiation upon the transmission of epidemic influenza in long-term hospital patients. *The American Review of Respiratory Disease* **83**, 36–38.
40. **Moser MR, *et al.*** (1979) An outbreak of influenza aboard a commercial airliner. *American Journal of Epidemiology* **110**, 1–6.
41. **Drinka PJ, *et al.*** (1996) Report of an outbreak: nursing home architecture and influenza-A attack rates. *Journal of the American Geriatrics Society* **44**, 910–913.
42. **Atkinson MP and Wein LM** (2008) Quantifying the routes of transmission for pandemic influenza. *Bulletin of Mathematical Biology* **70**, 820–867.
43. **Lei H, *et al.*** (2018) Route of transmission of influenza A H1N1, SARS CoV and norovirus in air cabins – a comparative analysis. *Indoor Air* **28**, 394–403.

44. **Hui DS, *et al.*** (2006) Noninvasive positive-pressure ventilation: an experimental model to assess air and particle dispersion. *Chest* **130**, 730–740.
45. **Hui DS, *et al.*** (2009) Exhaled air and aerosolized droplet dispersion during application of a jet nebulizer. *Chest* **135**, 648–654.
46. **Hui DS, *et al.*** (2009) Exhaled air dispersion distances during noninvasive ventilation via different respironics face masks. *Chest* **136**, 998–1005.
47. **Wolff MH, *et al.*** (2005) Environmental survival and microbicide inactivation of coronaviruses. In Schmidt A, Wolff MH and Weber O (eds), *Coronaviruses with Special Emphasis on First Insights Concerning SARS*. Basel: Birkhäuser, pp. 201–212.
48. **Baker MG, *et al.*** (2010) Transmission of pandemic A/H1N1 2009 influenza on passenger aircraft: retrospective cohort study. *BMJ* **340**, c2424.
49. **Stehlé J, *et al.*** (2011) High-resolution measurements of face-to-face contact patterns in a primary school. *PLoS ONE* **6**, e23176.
50. **Voirin N, *et al.*** (2015) Combining high-resolution contact data with virological data to investigate influenza transmission in a tertiary care hospital. *Infection Control & Hospital Epidemiology* **36**, 254–260.

https://doi.org/10.1017/S0950268818001012